DOI: https://doi.org/10.17816/morph.688357 EDN: SWEGOV

Structural and Ultrastructural Changes in Striated Skeletal Muscle Tissue Following High-Energy Injuries in the Early Post-Traumatic Period

Pavel A. Zakharov[1], Alena A. Ovchinnikova[1], Yaroslav D. Tolkachev[1], Nikita S. Gladyshev[1], Maria S. Pecherskaya[2], Aleksey M. Emelin[1], Igor S. Limaev[1], Anton S. Buchaka[1], Irina A. Chekmareva[2], Maria A. Kozlova[1], David A. Areshidze[1], Marina A. Shchedrina[3], Igor E. Onnitsev[3], Roman V. Deev[1]

[1]Petrovsky National Research Centre of Surgery, Moscow, Russia;
[2]A.V. Vishnevsky National Medical Research Center of Surgery, Moscow, Russia;
[3]Main Military Clinical Hospital named after academician N.N. Burdenko, Moscow, Russia

ABSTRACT

BACKGROUND: With the sharp increase in mine-explosive injuries, one of the key tasks of modern histology is to assess the morphogenesis of high-energy limb tissue damage.

AIM: This study aimed to characterize striated skeletal muscle tissue in the zone of mine-explosive limb segment avulsion during the early post-traumatic period (days 1–4).

METHODS: Histological methods (hematoxylin and eosin staining and Martius Scarlet Blue [MSB] staining for fibrin age determination), immunohistochemical and immunofluorescence techniques (antibodies to CD3, CD20, CD31 [Platelet Endothelial Cell Adhesion Molecule-1], CD68, and NETs [Neutrophil Extracellular Traps]), transmission electron microscopy, and morphometric analyses were applied.

RESULTS: Post-traumatic pathological changes affected both muscle tissue (necrosis, fiber fragmentation, traumatic edema) and endomysial and perimysial connective tissue (traumatic edema, fibrin infiltration). Disruption of the cytoskeletal structure (sarcomeres), loss of myosatellite cells, and endothelial cell death in capillaries were observed. Local hemodynamic disturbances manifested as mosaic thrombosis, embolism, and hemorrhage. Within the first 24 hours, arterial and arteriolar spasms led to reduced tissue perfusion. Partial resolution of the spasms by day 4 likely corresponded to the second stage of traumatic shock (the torpid phase). Among leukocytes, $CD68^+$ macrophages were the first to respond, with extravasation beginning on day 2 after injury. A similar trend was observed for $CD3^+$ T cells. $CD20^+$ B cells showed no morphological signs of reactivity during this period. NET formation was observed both intravascularly and in the extravascular compartment.

CONCLUSION: Structural and ultrastructural changes in skeletal muscle tissue within the first 4 days after mine-explosive injury have been characterized.

Keywords: muscle tissue; mine-explosive injury; trauma; damage; electron microscopy; Kernohan index; Wagenvoort index.

To cite this article:
Zakharov PA, Ovchinnikova AA, Tolkachev YaD, Gladyshev NS, Pecherskaya MS, Emelin AM, Limaev IS, Buchaka AS, Chekmareva IA, Kozlova MA, Areshidze DA, Shchedrina MA, Onnitsev IE, Deev RV. Structural and Ultrastructural Changes in Striated Skeletal Muscle Tissue Following High-Energy Injuries in the Early Post-Traumatic Period. *Morphology*. 2025;163(4):363–377. DOI: 10.17816/morph.688357 EDN: SWEGOV

Submitted: 27.07.2025 **Accepted:** 02.08.2025 **Published online:** 09.09.2025

DOI: https://doi.org/10.17816/morph.688357 EDN: SWEGOV

Структурные и ультраструктурные изменения поперечно-полосатой скелетной мышечной ткани после высокоэнергетических повреждений в ранний посттравматический период

П.А. Захаров[1], А.А. Овчинникова[1], Я.Д. Толкачев[1], Н.С. Гладышев[1], М.С. Печерская[2], А.М. Емелин[1], И.С. Лимаев[1], А.С. Бучака[1], И.А. Чекмарева[2], М.А. Козлова[1], Д.А. Арешидзе[1], М.А. Щедрина[3], И.Е. Онницев[3], Р.В. Деев[1]

[1]Российский научный центр хирургии им. акад. Б.В. Петровского, Москва, Россия;
[2]Национальный медицинский исследовательский центр хирургии им. А.В. Вишневского, Москва, Россия;
[3]Главный военный клинический госпиталь им. Н.Н. Бурденко, Москва, Россия

АННОТАЦИЯ

Обоснование. В связи с резким увеличением числа минно-взрывных ранений одной из важных задач современной гистологии становится оценка морфогенеза высокоэнергетических повреждений тканей конечностей.

Цель — охарактеризовать поперечно-полосатую скелетную мышечную ткань в зоне минно-взрывного отрыва части сегмента конечности в ранний посттравматический период (1–4 суток).

Методы. Применены гистологические [окраска гематоксилином и эозином и окраска на давность образования фибрина MSB (Martius Scarlet Blue — окраска по Марццу, Скарлетт и Блю)], иммуногистохимические и иммунофлуоресцентный методы [антитела к CD3, CD20, CD31 (Platelet Endothelial Cell Adhesion Molecule-1), CD68, NETs (Neutrophil Extracellular Traps)], трансмиссионная электронная микроскопия, морфометрические методы исследования.

Результаты. Установлено, что после травмы патологические изменения затрагивают как мышечную ткань (некроз, фрагментация мышечных волокон, травматический отёк), так и соединительную ткань эндомизия и перимизия (травматический отёк, пропитывание фибрином). Показано нарушение структуры цитоскелета (саркомеров) мышечных волокон, гибель миостателлитоцитов и эндотелиоцитов капилляров. Нарушения местной гемодинамики проявляются мозаичными тромбозами, эмболией и кровоизлияниями. В первые сутки после ранения наблюдали спазм артерий и артериол, приводящий к снижению тканевой перфузии. Спазм частично разрешается к 4-м суткам после травмы, что, вероятно, связано с развитием II периода травматической болезни (торпидная фаза травматического шока). Среди лейкоцитов первыми реагируют $CD68^+$ макрофаги, что проявляется их экстравазацией начиная со 2-х суток после травмы. Аналогичная тенденция установлена и для $CD3^+$ Т-лимфоцитов. $CD20^+$ В-лимфоциты в указанные сроки не проявили морфологических признаков реактивности. Показано формирование NETs как в сосудах, так и во внесосудистом компартменте.

Заключение. Таким образом, охарактеризованы структурные и ультраструктурные изменения мышц в первые 4 суток после минно-взрывного повреждения.

Ключевые слова: мышечная ткань; минно-взрывная травма; травма; повреждение; электронная микроскопия; индекс Керногана; индекс Вагенворта.

Как цитировать:
Захаров П.А., Овчинникова А.А., Толкачев Я.Д., Гладышев Н.С., Печерская М.С., Емелин А.М., Лимаев И.С., Бучака А.С., Чекмарева И.А., Козлова М.А., Арешидзе Д.А., Щедрина М.А., Онницев И.Е., Деев Р.В. Структурные и ультраструктурные изменения поперечно-полосатой скелетной мышечной ткани после высокоэнергетических повреждений в ранний посттравматический период // Морфология. 2025. Т. 163, № 4. С. 363–377. DOI: 10.17816/morph.688357 EDN: SWEGOV

Рукопись получена: 27.07.2025 **Рукопись одобрена:** 02.08.2025 **Опубликована online:** 09.09.2025

DOI: https://doi.org/10.17816/morph.688357 EDN: SWEGOV

横纹骨骼肌组织在高能量损伤后早期创伤期的结构与超微结构变化

Pavel A. Zakharov[1], Alena A. Ovchinnikova[1], Yaroslav D. Tolkachev[1], Nikita S. Gladyshev[1], Maria S. Pecherskaya[2], Aleksey M. Emelin[1], Igor S. Limaev[1], Anton S. Buchaka[1], Irina A. Chekmareva[2], Maria A. Kozlova[1], David A. Areshidze[1], Marina A. Shchedrina[3], Igor E. Onnitsev[3], Roman V. Deev[1]

[1]Petrovsky National Research Centre of Surgery, Moscow, Russia;
[2]A.V. Vishnevsky National Medical Research Center of Surgery, Moscow, Russia;
[3]Main Military Clinical Hospital named after academician N.N. Burdenko, Moscow, Russia

摘要

论证。随着地雷爆炸伤数量的急剧增加，评估肢体组织高能量损伤的形态发生学特征成为当代组织学的重要任务之一。

目的。 描述在早期创伤期（1–4 天）地雷爆炸致肢体节段缺损区域内横纹骨骼肌组织的变化。

方法。采用组织学方法[苏木精–伊红染色；MSB（三色法，Martius Scarlet Blue）纤维蛋白染色]、免疫组化及免疫荧光方法[CD3、CD20、CD31（Platelet Endothelial Cell Adhesion Molecule–1）、CD68、NETs（Neutrophil Extracellular Traps）]，并结合透射电子显微镜及形态计量学方法进行研究。

结果。发现创伤后病理性改变既累及肌肉组织（坏死、肌纤维断裂、创伤性水肿），也波及内肌膜及肌束膜结缔组织（创伤性水肿、纤维蛋白渗出）。肌纤维细胞骨架（肌小节）结构受损，卫星细胞及毛细血管内皮细胞死亡。局部血流动力学紊乱表现为灶性血栓、栓塞及出血。创伤后第1天观察到小动脉及微动脉痉挛，导致组织灌注下降。至第4天痉挛部分缓解，可能与创伤病 II 期（休克迟钝期）的发展有关。在白细胞反应中，$CD68^+$巨噬细胞最早反应，自创伤后第2天开始发生血管外渗。$CD3^+$ T淋巴细胞呈现类似趋势。$CD20^+$ B淋巴细胞在此阶段未表现出形态学反应性。NETs的形成既见于血管内，也见于血管外间隙。

结论。本研究在地雷爆炸伤后前4天内，对骨骼肌的结构与超微结构变化进行了表征。

关键词：肌肉组织；地雷爆炸伤；创伤；损伤；电子显微镜；Kernohan指数；Wagenvoort指数.

To cite this article:
Zakharov PA, Ovchinnikova AA, Tolkachev YaD, Gladyshev NS, Pecherskaya MS, Emelin AM, Limaev IS, Buchaka AS, Chekmareva IA, Kozlova MA, Areshidze DA, Shchedrina MA, Onnitsev IE, Deev RV. 横纹骨骼肌组织在高能量损伤后早期创伤期的结构与超微结构变化. *Morphology*. 2025;163(4):363–377. DOI: 10.17816/morph.688357 EDN: SWEGOV

收到：27.07.2025 **接受：**02.08.2025 **发布日期：**09.09.2025

BACKGROUND

The assessment of tissue damage and regeneration patterns following high-energy impacts on the human body has become a highly relevant field of histology [1]. Such studies acquire particular practical significance during armed conflicts, when their results directly influence the diagnostic and therapeutic strategies of physicians across various specialties [2, 3]. High-energy, primarily gunshot injuries, have been extensively investigated using both experimental and clinical materials [4–7]. In cases of ordinary mechanical trauma and gunshot wounds, specific features of regenerative histogenesis in skin, striated skeletal muscle, and bone tissues have been established [1, 4, 7, 8]. A clinical morphological analysis of internal organ injuries in servicemen, both local and systemic, provided the basis for the so-called hemodynamic concept of trauma response [6, 8]. According to this concept, the extent of ischemic necrosis resulting from post-traumatic microcirculatory disorders and subsequent replacement of functional parenchyma by connective tissue is determined not only by the initial structural damage at the moment of injury but also by pathological vasomotor reactions at the microcirculatory level, leading to functional failure of internal organs.

Researchers note that the ratio of different types of combat injuries varies depending on the tactical conditions in a particular theater of military operations [2, 9], with mine-blast injuries increasingly prevailing in recent years. Despite this, the morphological analysis of limb tissues under this type of high-energy injury remain insufficiently studied.

Unlike gunshot or shrapnel wounds, a mine-blast injury is considered a combined injury. It results from the cumulative action of a brisant gas–dust jet (a wave of detonation gases and the blast wave), a shock wave that causes contusive–commotional tissue damage, and the effects of fragments, flame, and toxic combustion products [6, 10]. This complex of damaging factors largely determines the specific morphology of mine-blast injuries and the extent of injury across body regions or limb segments. In particular, in cases of mine-blast limb detachments, it is impossible to identify the well-known zonality of the wound channel described for gunshot and shrapnel injuries, since no such wound canal exists [8]. Several morphological regularities of wound process in mine-blast injuries have been described [5, 11]. However, current data remain insufficient to fully characterize the sequence of events underlying the first and second stages of trauma response—specifically, the mechanisms of primary and secondary necrosis, delayed programmed cell death, infectious complications, and both local and systemic immune responses [6, 8, 11].

The work aimed to characterize the striated skeletal muscle tissue in the zone of a mine-blast detachment of a part of a limb segment in the early post-traumatic period (1–4 days).

METHODS

Study Setting

The study was conducted under a scientific collaboration agreement with the N.N. Burdenko Main Military Clinical Hospital.

Eligibility Criteria

The study included 31 samples of skeletal muscle tissue obtained during primary surgical debridement of the lower limb stump following mine-blast–related detachment of limb segments. Tissue alterations were analyzed 1–4 days post-injury.

Inclusion criteria: patients aged 18–65 years; traumatic injury accompanied by complete or partial detachment of a limb; amputation performed during primary surgical debridement within 1–6 cm from the detachment line; written informed consent.

Exclusion criteria: systemic diseases (such as diabetes mellitus, atherosclerosis of the lower limb arteries, HIV infection, or viral hepatitis B or C) and malignant neoplasms.

Intervention

Samples were obtained intraoperatively during primary surgical debridement of the amputated limb stump from four distinct sites: directly at the detachment line and 2, 4, and 6 cm proximally along the limb segment. All collected specimens were fixed in 10% formalin, followed by standard histological processing and embedding in paraffin blocks. Serial 4-μm sections were prepared and stained with hematoxylin and eosin (MLT, Russia), as well as for fibrin using Martius Scarlet Blue (MSB; ErgoProduction LLC, Russia). The perimeter and cross-sectional area of muscle fibers were measured quantitatively. To assess muscle perfusion, two complementary indices were calculated: the Wagenvoort index (the ratio of arterial wall area to lumen area) and the Kernohan index (the ratio of vascular wall thickness to lumen diameter) [12, 13].

Cells of the inflammatory infiltrate were identified immunohistochemically using antibodies to CD3 for the detection of T cells (dilution 1:75; cat. No. MRQ-39, Cell Marque, USA), CD20 for the detection of B cells (1:100; cat. No. L26, Cell Marque, USA), and CD68 for the detection of macrophages (1:100; cat. No. PG-M1, Dako, USA). For the immunohistochemical identification of vascular endothelium, antibodies to CD31 (Platelet Endothelial Cell Adhesion Molecule-1; dilution 1:50; cat. No. JC70, Cell Marque, USA) were used. All reactions were performed automatically using a Bond III instrument (Leica Biosystems, USA).

Detection of neutrophil extracellular traps (NETs) was performed on skeletal muscle sections obtained 2 and 6 cm proximally from the detachment line. Primary antibodies against fibrinogen (1:1000; cat. No. ab118533, Abcam, UK) and myeloperoxidase (1:500; cat. No. ab9535, Abcam, UK) were used. Detection systems included antibodies conjugated

with Alexa Fluor 488 (1:500; cat. No. ab150105, Abcam, UK) and Alexa Fluor 405 (1:500; cat. No. ab175676, Abcam, UK). The samples were examined under a semi-motorized upright fluorescence microscope Olympus BX53 (Olympus Corporation, Japan) using reflected-light fluorescence in the blue and green spectral ranges, followed by image processing by overlaying two channels.

For transmission electron microscopy, immediately after surgery (amputation), a fragment of muscle tissue of approximately 1 mm^3 in size was excised directly in the operating room and fixed in 2.5% glutaraldehyde solution in phosphate buffer (pH 7.4). The samples were then post-fixed in 1% osmium tetroxide, dehydrated in ethanol, contrasted with 1% uranyl acetate in 70% ethanol, and embedded in an epon–araldite mixture. Semi-thin sections were stained with methylene blue (Scientific Research Center for Pharmacotherapy, Russia). Ultrathin sections obtained with a UC Enuity ultramicrotome (Leica Microsystems, Germany) were additionally contrasted with lead citrate according to Reynolds. Microscopy was performed using a field-emission transmission electron microscope Himera EM50X (Ciqutek, China).

Statistical Analysis

Statistical analysis was performed in R (v. 4.4.1; R Foundation for Statistical Computing) using the tidyverse, rlang, purrr, and flextable packages. For each quantitative variable, the median and interquartile range (M [Q1; Q3]) were calculated separately for each observation day (days 1, 2, and 4) and for each distance from the detachment line (0, 2, 4, and 6 cm).

Intergroup comparisons were performed using the nonparametric Kruskal–Wallis test; two-sided p-values < 0.05 were considered significant.

RESULTS

On the first day after injury, muscle fibers along the detachment line had completely lost their transverse striation and, in several areas, showed fragmentation. In the marginal zones, distinct carbonization was observed; skin flaps were found adjacent to the muscle tissue, and foreign bodies such as plant debris and soot particles were present within the tissue. In cross-sections, muscle fibers appeared disconnected, the endomysium was markedly altered, and interfiber spaces were filled with loose fibrin masses (see Fig. 1, *a*). The fibrin impregnation was diffuse and extensive, containing occasional leukocytes and erythrocytes. When determining the age of fibrin deposits, both young (4–6 hours) and mature fibrin areas could be detected within the same specimen (see Figs. 1*c*–1*f*).

Blood vessels demonstrated pronounced spasm not only in small arteries and arterioles (see Fig. 2) but also in veins. Characteristic findings included fibrin and hyaline thrombi within the lumina of small vessels. Optically empty vacuoles observed in some vascular lumina indicated fat and/or air embolism.

At a depth of 2 cm from the detachment line, fragmented muscle fibers showed partial loss of nuclei. Fibrin masses in the endomysium contained numerous erythrocytes, indicating hemorrhagic impregnation of the muscle tissue. The color

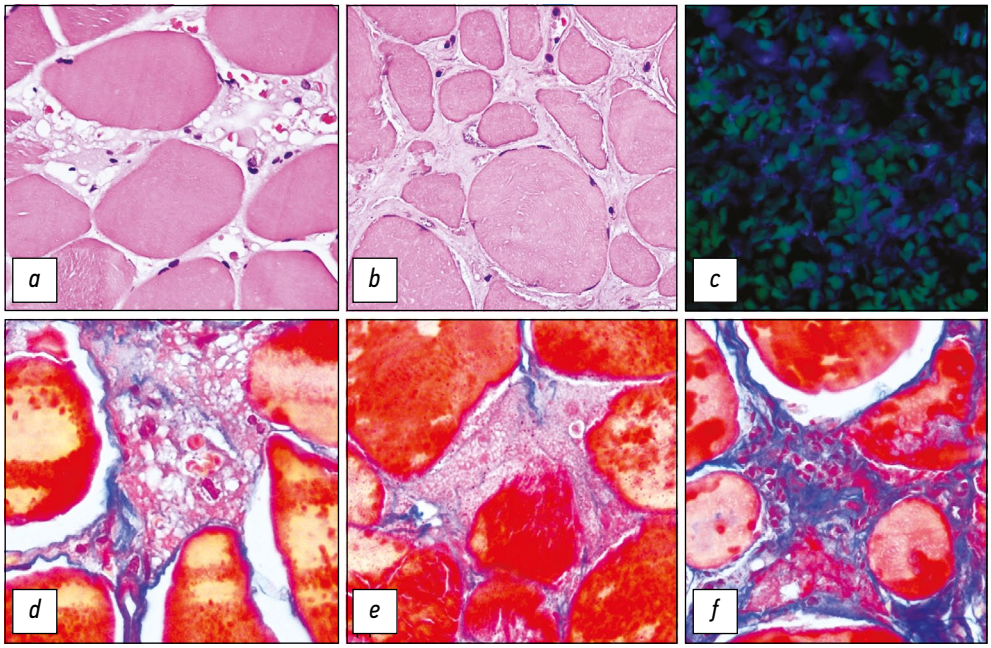

Fig. 1. Fibrin in the interstitial fluid of the endomysium: *a*, skeletal muscle tissue at the site of limb avulsion, 1 day after injury; *b*, skeletal muscle tissue at the site of limb avulsion, 4 days after injury; *c*, fibrinogen (blue) in the endomysium, 2 cm from the avulsion line, 1 day after injury. Fibrin in the endomysial exudate: *d*, *e*, fibrin in the endomysial exudate corresponding to an interval of up to 12 hours; *f*, fibrin in the endomysial exudate corresponding to 18–24 hours. Staining: *a*, *b*, hematoxylin and eosin; c, immunofluorescence with antibodies to fibrinogen (Alexa Fluor 405); *d*–*f*, Martius Scarlet Blue. Magnification: *a*, *b*, *d*–*f*, ×400; *c*, ×50.

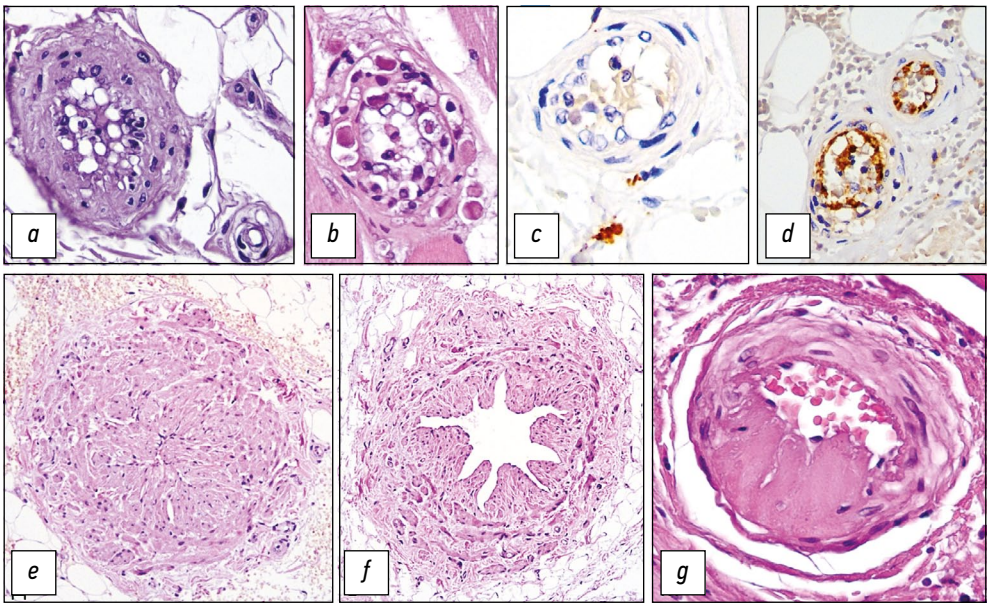

Fig. 2. Endomysial and perimysial arteries, 1 day after injury, 2–4 cm from the avulsion line: *a*, air and/or fat embolism, endothelial desquamation; *b*, vascular wall and cellular edema, endothelial desquamation; *c*, *d*, partial lumen occlusion by desquamated endothelial cells; *e*, *f*, arterial spasm; *g*, partial (semicircular) necrosis and edema of the vascular wall, dissection of the tunica adventitia. Staining: *a*, *b*, *e*–*g*, hematoxylin and eosin; *c*, immunohistochemistry with CD68 antibodies; *d*, immunohistochemistry with CD31 antibodies. Magnification: *a*–*d*, *g*, ×400; *e*, *f*, ×100.

of fibrin on MSB staining corresponded to an estimated age of 18–24 hours, which matched the timing of injury. In some areas, both the fibrin network and endomysial matrix appeared loosened due to edema. Isolated findings included intrafibrillar hemorrhages (see Fig. 3*a*). In addition, this region was characterized by partial necrosis (destruction) of muscle fibers, with the necrotic zones filled with fine-granular material (see Figs. 3*b,* 3*c*).

Some blood vessels, without a clear topographic pattern relative to the detachment line, exhibited vasospasm. In the lumina of several vessels, emboli (optically empty vacuoles) were observed, consisting of air bubbles, fat droplets, and desquamated endothelial cells (see Fig. 2*d*). In certain cases, edema and partial necrosis of the vascular wall were noted, along with asymmetric spasm. Immunofluorescent colocalization of fibrinogen and myeloperoxidase (NETs) revealed positive signals among sludged erythrocytes within the small vessels of the examined region.

Ultrastructural signs of damage were highly heterogeneous. In some marginal areas, coagulated tissues were identified. Within muscle fibers, disorganization of sarcomeric elements was verified, manifested by shortened distances between Z-lines and loss of clear boundaries between A- and I-bands. The sarcoplasmic reticulum and

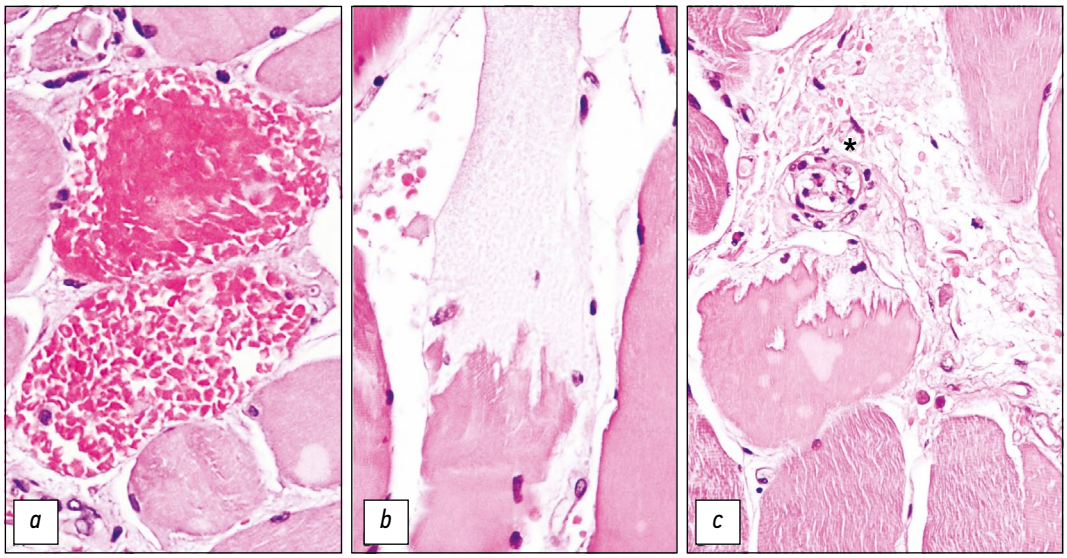

Fig. 3. Damage to striated skeletal muscle tissue (cross-section), 1 day after injury, 2 cm from the avulsion line: *a*, intrafibrillar hemorrhages; *b*, *c*, partial destruction of muscle fibers; * denotes an occluded blood vessel with wall edema. Hematoxylin and eosin staining; magnification ×400.

mitochondria appeared vacuolated, the latter containing single, disoriented short cristae within an electron-lucent matrix. Death of myosatellite cells was characteristic, evidenced by a marked reduction in the volume of vacuolated cytoplasm, disappearance of organelles, plasmolemmal rupture, and the presence of a large, invaginated nucleus with dense chromatin clumps along the nucleolemma (see Fig. 4*a*). In other fields, myosatellite and stromal cells exhibited a more electron-lucent cytoplasm. Occasionally, localized dilations of the perinuclear space and small chromatin aggregates in otherwise light nuclei were observed (see Figs. 4*b,* 5*a*). The cytoplasm contained dilated cisternae of the rough endoplasmic reticulum and heteromorphic, often edematous mitochondria, with extensive plasmolemmal disruption.

At the cytoskeletal level, muscle fibers frequently demonstrated disorganization of A- and I-bands and loss of Z-lines (see Fig. 4*c*). Some fibers showed fragmentation of myofibrils with the normal alignment of Z-lines and associated triads (see Fig. 5*b*). In the rarefied subsarcolemmal space, flocculent debris was observed. Intermyofibrillar regions contained swollen, vacuolated mitochondria with an electron-lucent matrix and residual cristae. The sarcoplasmic reticulum was vacuolated. Microvascular structures demonstrated marked vascular wall edema and luminal narrowing, as well as pronounced perivascular edema, destruction of endothelial cells (cytoplasmic and organelle lysis), and death of pericytes.

At a distance of 4–6 cm from the detachment line, the muscle tissue showed a mosaic alternation of destroyed muscle fibers, hemorrhagic impregnation, and moderate leukocytic infiltration. In this region, extravasation of polymorphonuclear leukocytes was observed. Most muscle fibers showed signs of sarcoplasmic material destruction (see Fig. 5). Vascular changes were stereotypical: arteries and arterioles exhibited spasm and a stellate lumen due to folding of the *tunica intima*; numerous leukocytes were visualized in small veins. Single $CD68^+$ macrophages and $CD3^+$ T cells were found in the endomysium, closely associated with muscle fibers or located perivascularly. $CD20^+$ B cells were extremely rare.

In samples obtained two days after injury, the growth of rod-shaped microorganisms was detected along the muscle tissue at the detachment line, without any reaction from the underlying tissues. The muscle tissue showed loss of nuclei and fragmentation of muscle fibers; the spaces between fiber fragments were filled with fibrin masses containing a few wandering cells. The phenomenon of free nuclei was noted in several fibers.

At a distance of 2 cm from the detachment line, the leukocytic reaction was more pronounced. Histocytic infiltration of the edematous perimysium, margination of macrophages in arteries, and their infiltration into vascular walls were observed (see Figs. 6*b,* 6*c*). Necrotized muscle fibers underwent phagocytosis by individual macrophages. Most arteries remained in spasm; fibrin and hyaline thrombi persisted, and signs of embolism could be detected. NETs were identified both within thrombotic masses and extravasally, in areas of hemorrhagic impregnation.

At a distance of 4–6 cm from the detachment line, there was massive hemorrhagic impregnation, fragmentation, and

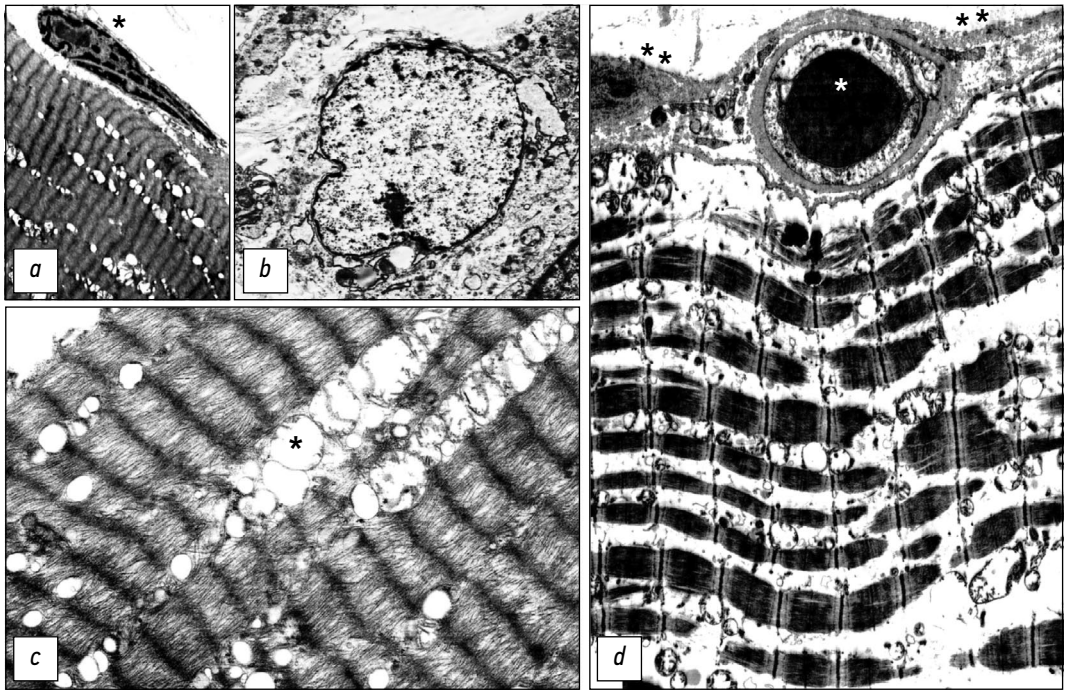

Fig. 4. Ultrastructural changes in striated skeletal muscle tissue, 1 day after injury, 2–4 cm from the avulsion line: *a*, fragment of a muscle fiber with destroyed mitochondria and a degenerated myosatellitocyte; *b*, destroyed endomysial cell; *c*, cytoskeleton of a muscle fiber, * indicates mitochondria undergoing destruction; *d*, fragment of a muscle fiber with disorganized myofibrils and destroyed mitochondria, * indicates a capillary with a red blood cell, ** indicates edematous basement membrane. Transmission electron microscopy, magnification: *a*, ×7000; *b*, ×7500; *c*, ×14,000; *d*, ×5500.

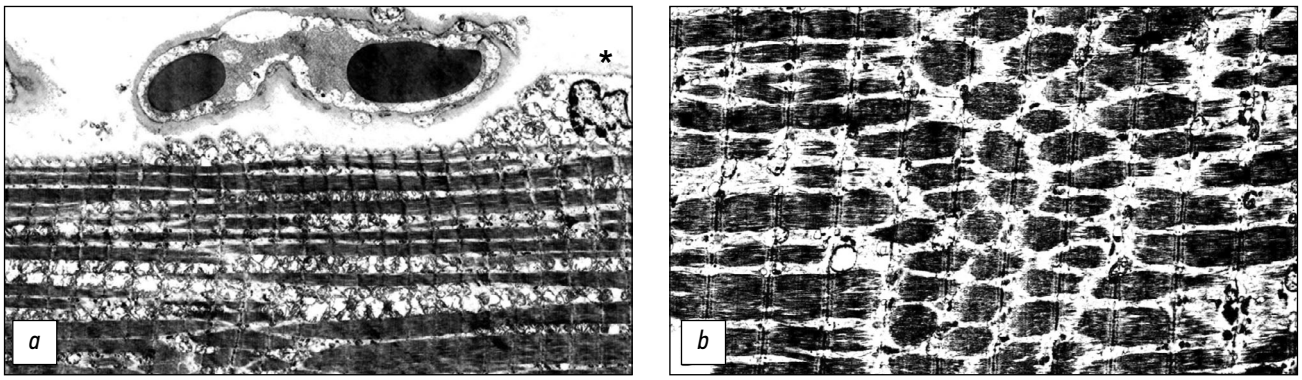

Fig. 5. Ultrastructural changes in striated skeletal muscle tissue, 1 day after injury, 4 cm from the avulsion line: *a*, fragment of a myosatellitocyte with a shrunken nucleus and destroyed mitochondria, * indicates red blood cells in the capillary lumen, partial myofibril destruction and total mitochondrial death; *b*, fragmentation of myofibrils, destruction of mitochondria and triads. Transmission electron microscopy, magnification: *a*, ×3000; *b*, ×7000.

destruction of muscle fibers, along with signs of autolysis. The leukocytic response was sparse.

The degree of intracellular edema in muscle fibers was assessed by measuring their perimeter and cross-sectional area at different time points after injury (see Tables 1, 2). A significant increase in these parameters was found between days 1 and 4 after injury. The severity of edema decreased with increasing distance from the detachment line (days 1 and 4).

On day 4 after injury, muscle tissue at the detachment line was intensively infiltrated with neutrophilic granulocytes, with areas of hemorrhagic impregnation. Fibrin deposited between muscle fibers appeared homogenized and compacted (Fig. 1*b*). Clusters of reactively altered connective tissue elements promoted the early stages of granulation tissue development (see Fig. 5*d*).

At a distance of 2 cm from the detachment line, pronounced autolysis of muscle tissue was observed, with massive fragmentation of muscle fibers. The tissue underwent lytic changes due to the accumulation of a leukocyte-rich exudate. Edema, destruction of collagen fibers, and dense leukocytic infiltration were observed in the connective tissue matrix of the endomysium and perimysium. Single myosymplasts of small diameter with intensely basophilic nuclei, arranged in rosettes or chains, were detected.

Changes in the vascular bed maintained a stereotypical pattern, including mosaic spasm of small arteries and arterioles, as well as embolic phenomena of decreasing

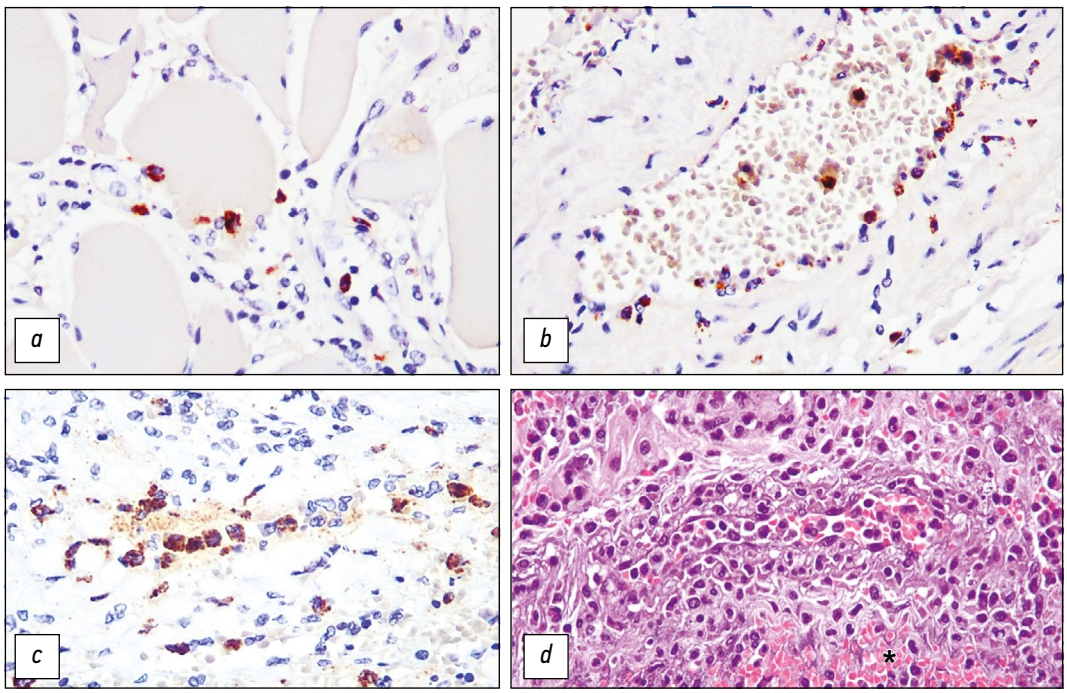

Fig. 6. Macrophages in the area of muscle tissue injury, 2–4 cm from the avulsion line: *a*, CD68+ macrophages in the endomysium and phagocytosis of a damaged muscle fiber, 1 day after injury; *b*, margination of monocytes/macrophages in an artery, 2 days after injury; *c*, monocytes/macrophages in a thin-walled endomysial vessel, 2 days after injury; d, monocytes/macrophages in the vascular lumen, within an infiltrate and organizing hemorrhage (*), 4 days after injury. Staining: *a–c*, immunohistochemistry with CD68 antibodies; *d*, hematoxylin and eosin. Magnification ×400.

severity. Perfusion indices showed significant changes depending both on the depth of injury and on the time since injury (see Tables 3, 4). The Wagenvoort index decreased from the day of injury, reaching its minimum value by day 4 at the maximum studied distance (6 cm) from the detachment line. The Kernohan index confirmed this trend.

At a distance of 4–6 cm from the detachment line, large tissue areas were disrupted by hemorrhages and regions containing lipid droplets with early signs of organization and massive leukocytic infiltration. Notably, hemosiderophages were absent. Thin-walled vessels actively delivered polymorphonuclear leukocytes to this zone. The arteries remained in a state of spasm. In several cases, the vascular wall was densely infiltrated with leukocytes from the *tunica externa*, indicating the onset of vasculitis; however, the vessels remained patent.

Given these findings, particular attention should be paid to the changes in leukocyte infiltration within the injury zones, which reflect both the potential for oxygenation and the capacity for leukocyte delivery.

The changes in $CD68^+$ macrophage counts indicated that the observed changes were of a diffuse–focal pattern and depended on the perfusion status of individual muscle tissue regions (see Table 5). The number of $CD68^+$ cells increased

Table 1. Perimeter of muscle fibers, μm

Distance from detachment line, cm	Time after injury, days			*p*-value
	1	2	4	
0	337.07 [282.62; 389.61]	283.55 [185.63; 473.36]	317.05 [265.28; 345.48]	0.0236
2	307.87 [245.18; 386.82]	293.54 [273.83; 351.16]	353.49 [331.95; 409.26]	0.0026
4	242.84 [204.42; 277.99]	297.29 [263.59; 341.02]	328.42 [288.61; 368.76]	0.0000
6	268.53 [237.25; 319.81]	319.57 [279.00; 369.38]	185.89 [130.31; 291.76]	0.0000
p-value	0.0000	0.2511	0.0000	-

Table 2. Cross-sectional area of muscle fibers, μm^2

Distance from detachment line, cm	Time after injury, days			*p*-value
	1	2	4	
0	6110.92 [4522.70; 7794.73]	4827.60 [2196.35; 10927.55]	6153.04 [4754.95; 7892.40]	0.1176
2	5855.90 [3731.12; 8834.94]	5297.20 [4492.88; 7397.70]	6753.65 [5821.00; 9009.75]	0.0660
4	3547.05 [2494.95; 4865.85]	5273.40 [4483.62; 7300.45]	6056.51 [4653.91; 7279.44]	0.0000
6	4212.80 [3279.70; 5636.91]	5866.90 [5212.62; 7903.38]	2330.50 [1066.10; 4992.25]	0.0000
p-value	0.0000	0.0787	0.0000	-

Table 3. Wagenvoort index

Distance from detachment line, cm	Time after injury, days			*p*-value
	1	2	4	
0	57.16 [47.52; 63.65]	50.23 [34.80; 57.16]	42.66 [36.64; 48.97]	0.0088
2	51.85 [35.92; 61.39]	41.16 [33.94; 56.62]	61.22 [55.41; 67.19]	0.0163
4	48.37 [35.58; 59.03]	49.33 [35.74; 59.05]	59.66 [46.39; 78.39]	0.3401
6	48.87 [40.76; 61.14]	43.59 [34.08; 50.59]	29.85 [25.57; 36.70]	0.0032
p-value	0.0166	0.8523	0.0001	-

Table 4. Kernohan index

Distance from detachment line, cm	Time after injury, days			*p*-value
	1	2	4	
0	1.33 [0.91; 1.75]	1.01 [0.54; 1.34]	0.75 [0.58; 0.96]	0.0088
2	1.08 [0.56; 1.60]	0.70 [0.51; 1.31]	1.58 [1.24; 2.06]	0.0163
4	0.94 [0.55; 1.44]	0.98 [0.56; 1.44]	1.48 [0.87; 3.63]	0.3401
6	0.96 [0.69; 1.57]	0.77 [0.52; 1.02]	0.43 [0.34; 0.58]	0.0032
p-value	0.0166	0.8523	0.0001	-

Table 5. Number of $CD68^+$ macrophages in tissues, per 1 mm^2

Distance from detachment line, cm	Time after injury, days			*p*-value
	1	2	4	
2	36.3 [19.8; 66.8]	19.8 [13.2; 30.5]	153.4 [115.5; 176.5]	0.000
6	64.3 [33.0; 90.7]	57.8 [28.9; 84.2]	82.5 [40.9; 258.6]	0.143
p-value	0.027	0.001	0.202	-

Table 6. Number of $CD3^+$ T cells in tissues, per 1 mm^2

Distance from detachment line, cm	Time after injury, days			*p*-value
	1	2	4	
2	9.9 [6.6; 19.8]	3.3 [0.8; 3.3]	23.1 [6.6; 37.9]	0.000
6	6.6 [3.3; 13.2]	8.2 [3.3; 13.2]	23.1 [13.2; 66.0]	0.000
p-value	0.032	0.005	0.281	-

with the distance from the detachment line and time since injury. Deviations from this pattern were likely due to the mosaic nature of tissue alterations and the uneven distribution of damaging factors and local perfusion disturbances.

A similar trend in expression was observed for T cells (see Table 6). $CD20^+$ B cells were detected only sporadically at all examined post-injury time points.

DISCUSSION

As aptly stated by Avtsyn, a wartime pathologist (1943–1945), "From a general biological point of view, a gunshot wound can briefly be described as a monstrous experiment on a human being by virtue of its brutality" [14]. It is generally accepted that in Russian medical practice, the particularly destructive consequences of high-energy trauma to tissues were first noted by Pirogov, who wrote: "What especially distinguishes, in my view, the effect of a projectile on tissues is precisely the molecular concussion it produces; its boundaries and extent we can never determine precisely" [15]. The morphological features of wound channels in gunshot and/or shrapnel injuries were described during World War I by the German pathologist Borst. He proposed the concept of the three-layer structure of the wound canal wall. Borst distinguished the following: a zone of tissue defect, associated with the impact of the primary shock wave and the projectile itself; a lateral wall, representing the zone of primary necrosis formed under the influence of the lateral shock wave (lateral impact); and a deeper zone of secondary necrosis, the development of which depends on microcirculatory disturbances within the affected tissues (in modern terminology) [16]. World War II and the subsequent decades brought new insights into wound ballistics and tissue responses to high-energy impacts. Fundamental contributions in this field were made by Soviet morphologists Davydovsky, Maksimenkov, Dyskin, and others [3, 10].

The experience of armed conflicts throughout the 20th and early 21st centuries has shown a steady increase in the proportion of mine-blast injuries among combat casualties [2, 8–11]. The injuring factors of mine-blast trauma render the resulting wound non-identical to a gunshot wound. In particular, the classical zoning pattern becomes less distinct. According to Klochkov et al. [8], a zone of primary traumatic necrosis (zone 1) without clear boundaries forms at the border of the detached limb segment. In surgical practice, this area has been referred to as the zone of detachment, crushing, and tissue separation. The extent of this zone may reach 5–35 cm [11]. Zone 1 transitions into the zone of contusional and commotional damage (zone 2), which can be conditionally regarded as the analog of the zone of secondary necrosis (lateral impact), characterized by vasomotor disturbances affecting the remaining part of the limb segment [8]. However, zone 2 may still contain areas of minimally altered or intact tissue [11]. The extent of both zones depends on several factors, including the type of ammunition, angle of explosive energy application, limb position, and other parameters [11].

In the present study, we examined areas of muscle tissue primarily corresponding to zone 1 and partially to zone 2 of mine-blast injury. Structural alterations of striated skeletal muscle tissue in regions adjacent to the border of the detached limb segment have been previously described, demonstrating that they may include the so-called stair-step pattern of muscle rupture [8]. In our research, fragmentation of muscle fibers was consistently detected in the presence of pronounced traumatic edema caused by fibrin-rich exudate, resulting in a distinct morphological pattern. Intracellular edema was confirmed by daily measurements of the muscle fiber perimeter and cross-sectional area (Tables 1, 2). These findings are consistent with reports that in the early post-traumatic period following high-energy injury, tissue changes are predominantly alterative and exudative [8, 17].

The mechanisms of tissue damage resulting from the gas-dust impact are described in scientific and educational publications using various terms. The concept of brisant (crushing) action is generally accepted. Together with

the shock wave, it is complemented by the description of additional mechanisms—splitting, inertial, and cavitation injuries [10]. Examinations of the tissues after injury indicate that the damaging factors act not only at the structural but also at the ultrastructural level, disrupting membranous and nonmembranous organelles, the cytoskeleton, and the cellular energy apparatus. Mitochondria, even under conditions of high-energy trauma, appear to remain among the organelles most sensitive to damage. It is likely that local perfusion disturbances—that is, hypoxic (secondary) injury—contribute to ultrastructural (molecular) damage.

The hydrodynamic impact generated by the propagation of the blast wave through the liquid phase (blood) within the vessels undoubtedly causes marked structural alterations in the vascular wall. Previous reports schematically depict shock-wave splitting injuries as longitudinal ruptures of the arterial *tunica intima* extending into the internal elastic membrane [11]. This phenomenon was not observed in our study. However, in our study, pronounced spasm of arteries and arterioles was repeatedly observed at various distances from the detachment line during the initial stage of trauma response (the primary neuroendocrine response to injury), leading to pronounced folding of the intimal and muscular layers. Perfusion index assessment demonstrated that, despite the diffuse-focal pattern of changes, generalized vasospasm serves as the morphological correlate of the immediate response to severe, often combined, trauma within the first 24 hours. By the fourth day post-injury, both Kernohan and Wagenvoort indices showed changes reflecting vessel lumen expansion and, in some cases, arterial wall thickening due to edema. This tendency is likely a manifestation of the second period of trauma response, corresponding to the torpid phase of traumatic shock, which is associated with the entry of autolytic products from large volumes of necrotizing tissues (fermentemia) into the systemic bloodstream, as well as with tissue hypoxia and acidosis [6, 8, 18]. At the same time, the muscles showed no complete vascular relaxation, with persistently spasmed arteries and arterioles remaining in a mosaic distribution across different compartments of the muscle.

An evaluation of the leukocytic response in tissues following high-energy trauma revealed several distinctive features. Numerous leukocytes in the venous bed had been noted previously [2]. Vayl regarded this phenomenon as reflexive [2]. The tissues at the detachment line, however, contained no phagocytic elements for a relatively long period (1–2 days) despite pronounced necrotic changes. This may be due to persistent disturbances of hemodynamics and vascular patency in this region. A delay in the progression of all phases of the wound process, from the formation and delimitation of necrosis to inflammatory changes, has also been reported previously [6, 17].

Specific signs of neutrophil death (NETs), both within the intravascular compartment (sludge, thrombi) and in hemorrhagic areas, may indicate a high level of microbial contamination following mine-blast injuries, as well as the activation of nonspecific defense mechanisms (innate immunity) already at the early stages of the wound process. It is known that possible triggers for neutrophil trap formation include bacterial, fungal, and viral infections, which can induce this type of neutrophil death through pathogen-associated molecular patterns (PAMPs) [19, 20]. In addition to the canonical pathway, a second mechanism of NET induction has been described, mediated by damage-associated molecular patterns (DAMPs). These include certain cytoplasmic and nuclear proteins, nucleic acids, and components of mitochondria, lysosomes, and others [20, 21]. The release of these molecules from deeply injured tissue structures after high-energy trauma is evident [22, 23]. NET release followed by thrombus formation can be regarded as a nonspecific protective response of tissues and the body as a whole, activated even before the onset of inflammation associated with microbial invasion.

No significant signs of purulent inflammation were detected during the study period following injury; the observed pattern indicated an alterative–exudative process. In areas with mosaic preservation of blood flow, monocyte–macrophage migration developed by days 2–4 after injury. A similar trend was observed for T cells, which, according to Sidorin [17], provide immunological support for reparative regeneration during the formation and subsequent remodeling of granulation tissue. The observed increase in B cells corresponded to later stages of the wound process [17].

Study Limitations

This study was conducted using tissue samples obtained from patients immediately after limb stump amputation performed during primary surgical debridement. When interpreting the findings, the authors proceeded from the assumption that, following severe combined high-energy trauma accompanied by acute massive blood loss and traumatic shock, patients were in a state of systemic response to injury. The individual degree of such a response, due to objective circumstances, could not be accounted for in each analyzed case. The influence of therapeutic interventions (analgesia, hemostasis, infusion therapy, and others) also remained beyond the scope of discussion, representing an important limitation of the present analysis.

CONCLUSION

The study demonstrated that during the early post-traumatic period (days 1–4) following high-energy limb injury (partial segment detachment), the affected tissues undergo changes that include traumatic edema with protein-rich fluid accumulation, progressive perfusion disturbances, and pronounced ultrastructural damage (molecular concussion). Under these conditions, a delay in innate immune and local lymphocytic responses predisposes to secondary necrosis and complications.

Understanding tissue reactions and hemodynamic patterns following mine-blast injuries contributes to identifying new pathogenetic targets in the treatment of wounded patients. In the vast majority of cases, such injuries are segmental [6, 8, 10, 11] and do not allow for tissue-sparing management; treatment in these situations follows the doctrine that amputation should be performed within tissues whose damage remains reversible [11]. Nevertheless, maintaining tissue viability and developing effective approaches for systemic drug delivery to injured regions are of a universal nature and may be applicable in relevant clinical settings.

ADDITIONAL INFORMATION

Author contributions: R.V. Deev, I.E. Onnitsev: conceptualization, investigation, writing—original draft; P.A. Zakharov, A.A. Ovchinnikova, Ya.D. Tolkachev, N.S. Gladyshev, M.S. Pecherskaya, A.M. Emelin, I.S. Limaev, A.S. Buchaka, I.A. Chekmareva, M.A. Kozlova, D.A. Areshidze, M.A. Shchedrina: investigation. All the authors approved the version of the manuscript to be published and agreed to be accountable for all aspects of the work, ensuring that questions related to the accuracy or integrity of any part of the work are appropriately investigated and resolved.

Ethics approval: The study was approved by the Local Ethics Committee of the Petrovsky National Research Centre of Surgery (Minutes No. 8, dated October 4, 2024).

Funding sources: This work was conducted as part of the state assignment "Pathomorphogenesis of mechanical and high-energy injuries of the musculoskeletal system and biotechnological methods of their correction" (FURG-2026-0035).

Disclosure of interests: The authors have no relationships, activities, or interests for the last three years related to for-profit or not-for-profit third parties whose interests may be affected by the content of the article.

Statement of originality: No previously obtained or published material (text, images, or data) was used in this study or article.

Data availability statement: All data obtained in this study are available in this article.

Generative AI: No generative artificial intelligence technologies were used to prepare this article.

Provenance and peer review: This paper was submitted unsolicited and reviewed following the standard procedure. The peer review process involved two external reviewers, a member of the Editorial Board, and the in-house scientific editor.

ДОПОЛНИТЕЛЬНАЯ ИНФОРМАЦИЯ

Вклад авторов. Р.В. Деев, И.Е. Онницев — определение концепции, проведение исследования, написание рукописи; П.А. Захаров, А.А. Овчинникова, Я.Д. Толкачев, Н.С. Гладышев, М.С. Печерская, А.М. Емелин, И.С. Лимаев, А.С. Бучака, И.А. Чекмарева, М.А. Козлова, Д.А. Арешидзе, М.А. Щедрина — проведение исследования. Все авторы одобрили рукопись (версию для публикации), а также согласились нести ответственность за все аспекты настоящей работы, гарантируя надлежащее рассмотрение и решение вопросов, связанных с точностью и добросовестностью любой её части.

Этическая экспертиза. Исследование одобрено локальным этическим комитетом ГНЦ РФ ФГБНУ «РНЦХ им. акад. Б.В. Петровского» (протокол № 8 от 04.10.2024).

Источники финансирования. Работа выполнена в рамках исполнения темы государственного задания «Патоморфогенез механических и высокоэнергетических повреждений структур опорно-двигательного аппарата и биотехнологические способы их коррекции» FURG-2026-0035.

Раскрытие интересов. Авторы заявляют об отсутствии отношений, деятельности и интересов за последние три года, связанных с третьими лицами (коммерческими и некоммерческими организациями), интересы которых могут быть затронуты содержанием статьи.

Оригинальность. При проведении исследования и создании настоящей статьи авторы не использовали ранее полученные и опубликованные сведения (данные, текст, иллюстрации).

Доступ к данным. Все данные, полученные в настоящем исследовании, представлены в статье.

Генеративный искусственный интеллект. При создании настоящей статьи технологии генеративного искусственного интеллекта не использовали.

Рассмотрение и рецензирование. Настоящая работа подана в журнал в инициативном порядке и рассмотрена по обычной процедуре. В рецензировании участвовали два внешних рецензента, член редакционной коллегии и научный редактор издания.

REFERENCES | СПИСОК ЛИТЕРАТУРЫ

1. Danilov RK. *Wound process: histogenetic bases*. Saint Petersburg: VMedA; 2007. (In Russ.)

2. Vail SS. *Materials on the pathological anatomy of combat trauma*. Kirov: Izdatel'stvo Voenno-morskoi meditsinskoi akademii; 1943. (In Russ.)

3. Davydovsky IV. *Human gunshot wound. Morphological and general pathological analysis*. Moscow: Izdatel'stvo AMN SSSR; 1952. (In Russ.)

4. Gololobov VG. *Bone tissue regeneration during healing of gunshot fractures*. Saint Petersburg: Peterburg–XXI vek; 1997. (In Russ.) ISBN: 5-88485-045-X

5. Nechaev EA, Gritsanov AB, Fomin NF, Minnullin IP. *Mine blast injury*. Saint Petersburg: Sankt-Peterburgskiy NIITO im. R. Vredena; 1997. (In Russ.)

6. Povzun SA, Gerasimov SM, Klochkov ND, et al. *Pathological anatomy of combat injuries and their complications*. Povzun SA, Klochkov ND, editors. Saint Petersburg: SM Kirov Military Medical Academy; 2002. (In Russ.)

7. Odintsova IA. *Regeneration histogenesis in skin-muscle wound* [dissertation]. Saint Petersburg; 2005. (In Russ.)

8. Klochkov ND, Povzun SA, Sidorin VS, et al. Pathological anatomy of combat trauma. In: *Experience of medical support of troops in Afghanistan 1979-1989. V 2. Organization and scope of surgical care*. Eryukhin IA, Khrupkin VI, editors. Moscow: NN Burdenko GVKG, 2002. P:68–131. (In Russ.)

9. Trishkin DV, Kryukov EV, Alekseev DE, et al. *Military field surgery. National guidelines*. Samokhvalov IM, editor. Moscow: GEOTAR-Media; 2024. (In Russ.) doi: 10.33029/9704-8036-6-VPX-2024-1-1056 ISBN: 978-5-9704-8036-6 EDN: AYGYWM

10. Nechaev EA, Gritsanov AI, Minnullin IP, et al. *Explosive injuries: A guide for doctors and students*. Nechaev EA, editor. Saint Petersburg: IKF «Foliant»; 2002. (In Russ.)

11. Wagenvoort CA, Wagenvoort N. Primary pulmonary hypertension: A pathologic study of the lung vessels in 156 clinically diagnosed cases. *Circulation*. 1970;42(6):1163–1184. doi: 10.1161/01.CIR.42.6.1163
12. Kernohan JW, Anderson EW, Keith NM. The arterioles in cases of hypertension. *Arch Intern Med*. 1929;44(3):395–423. doi: 10.1001/archinte.1929.00140030094010
13. Avtsyn AP. *Essays on military pathology*. Moscow: Medgiz; 1946. (In Russ.)
14. Pirogov NI. Military medical care and private assistance in the theater of war in Bulgaria and in the rear of the active army in 1877-1878. In: *Pirogov NI. Collected Works*. Moscow: Medgiz; 1960. (In Russ.)
15. Borst M. Algemeines uber die Wirkung der Geschosse, Waffen. In: *Hand. d. Arcitl. Erfahrungen im Weltkriege 1914-1918* Jahr. Bd. 8. Leipzig; 1921. S:206–235. (In German)
16. Fomin NF. The contribution of surgeons-anatomists of the Military Medical Academy to the study of mechanogenesis and morphology of combat surgical trauma. In: *Proceedings of the All-Russian scientific and practical conference «Anatomical, physiological and clinical-morphological aspects of modern high-energy injuries»*, Saint Petersburg, 2024 Nov 11. Saint Petersburg: VMedA; 2024. P. 5–18. EDN: ZUPMKW
17. Sidorin *VS. Pathomorphology of the immune system in traumatic disease in the wounded* [dissertation]. Saint Petersburg; 1993. (In Russ.)
18. Povzun SA. Wounds and wound process. Traumatic, radiation and burn diseases. In: *Pathological anatomy: national guidelines.* Paltsev MA, Kaktursky LV, Zairatyants OV, editors. Moscow: GEOTAR-Media; 2011. P:1162–1186 (In Russ.)
19. Papayannopoulos V. Neutrophil extracellular traps in immunity and disease. *Nat Rev Immunol*. 2018;18(2):134–147. doi: 10.1038/nri.2017.105 EDN: YFDICD
20. Bhatia N, George B, Masih D, et al. Mechanistic insights into PAMP and DAMP driven activation of NETosis in autoimmune disorders. *Int Immunopharmacol*. 2025;162:115149. doi: 10.1016/j.intimp.2025.115149
21. Chen T, Li Y, Sun R, et al. Receptor-mediated NETosis on neutrophils. *Front Immunol*. 2021;12:775267. doi: 10.3389/fimmu.2021.775267 EDN: OZLLHQ
22. Relja B, Land WG. Damage-associated molecular patterns in trauma. *Eur J Trauma Emerg Surg*. 2020;46(4):751–775. doi: 10.1007/s00068-019-01235-w EDN: GVLJJO
23. Pantalone D, Bergamini C, Martellucci J, et al. The Role of DAMPS in burns and hemorrhagic shock immune response: Pathophysiology and clinical issues. Review. *Int J Mol Sci*. 2021;22(13):7020. doi: 10.3390/ijms22137020 EDN: OYNNGJ

AUTHORS' INFO

***Roman V. Deev,** Cand. Sci. (Medicine), Assistant Professor;
address: 3 Tsyurupy st, Moscow, Russia, 117418;
ORCID: 0000-0001-8389-3841;
eLibrary SPIN: 2957-1687;
e-mail: romdey@gmail.com

Pavel A. Zakharov;
ORCID: 0009-0005-0425-9532;
e-mail: P.zakharov2510@gmail.com

Alena A. Ovchinnikova;
ORCID: 0009-0005-7610-998X;
e-mail: ovchinnikova_aa@student.med.ru

Yaroslav D. Tolkachev;
ORCID: 0009-0006-5188-1890;
e-mail: yaroslav.tolkachev.06@mail.ru

Nikita S. Gladyshev;
ORCID: 0000-0003-2732-5676;
eLibrary SPIN: 1852-6469;
e-mail: krinege@mail.ru

Maria S. Pecherskaya;
ORCID: 0000-0003-0835-1545;
eLibrary SPIN: 7410-1681;
e-mail: dr.uskova@mail.ru

Aleksey M. Emelin;
ORCID: 0000-0003-4109-0105;
eLibrary SPIN: 5605-1140;
e-mail: eamar40rn@gmail.com

Igor S. Limaev;
ORCID: 0000-0002-0994-9787;
eLibrary SPIN: 4909-6550;
e-mail: ig.limaev@gmail.com

ОБ АВТОРАХ

***Деев Роман Вадимович,** канд. мед. наук, доцент;
адрес: Россия, 117418, Москва, ул. Цюрупы, д. 3;
ORCID: 0000-0001-8389-3841;
eLibrary SPIN: 2957-1687;
e-mail: romdey@gmail.com

Захаров Павел Андреевич;
ORCID: 0009-0005-0425-9532;
e-mail: P.zakharov2510@gmail.com

Овчинникова Алёна Андреевна;
ORCID: 0009-0005-7610-998X;
e-mail: ovchinnikova_aa@student.med.ru

Толкачев Ярослав Дмитриевич;
ORCID: 0009-0006-5188-1890;
e-mail: yaroslav.tolkachev.06@mail.ru

Гладышев Никита Сергеевич;
ORCID: 0000-0003-2732-5676;
eLibrary SPIN: 1852-6469;
e-mail: krinege@mail.ru

Печерская Мария Сергеевна;
ORCID: 0000-0003-0835-1545;
eLibrary SPIN: 7410-1681;
e-mail: dr.uskova@mail.ru

Емелин Алексей Михайлович;
ORCID: 0000-0003-4109-0105;
eLibrary SPIN: 5605-1140;
e-mail: eamar40rn@gmail.com

Лимаев Игорь Сергеевич;
ORCID: 0000-0002-0994-9787;
eLibrary SPIN: 4909-6550;
e-mail: ig.limaev@gmail.com

* Corresponding author / Автор, ответственный за переписку

Anton S. Buchaka;
ORCID: 0000-0003-3580-1492;
eLibrary SPIN: 2416-2075;
e-mail: abpao62@yandex.ru

Irina A. Chekmareva, Dr. Sci. (Biology);
ORCID: 0000-0003-0126-4473;
eLibrary SPIN: 5994-7650;
e-mail: chia236@mail.ru

Maria A. Kozlova, Cand. Sci. (Biology);
ORCID: 0000-0001-6251-2560;
eLibrary SPIN: 5647-1372;
e-mail: ma.kozlova2021@outlook.com

David A. Areshidze, Cand. Sci. (Biology);
ORCID: 0000-0003-3006-6281;
eLibrary SPIN: 4348-6781;
e-mail: labcelpat@mail.ru

Marina A. Shchedrina, Cand. Sci. (Medicine);
ORCID: 0000-0002-4265-012X;
eLibrary SPIN: 1441-7163;
e-mail: Schcedrina-m@mail.ru

Igor E. Onnitsev, Dr. Sci. (Medicine);
ORCID: 0000-0002-3858-2371;
eLibrary SPIN: 9659-4740;
e-mail: ionnicev@mail.ru

Бучака Антон Сергеевич;
ORCID: 0000-0003-3580-1492;
eLibrary SPIN: 2416-2075;
e-mail: abpao62@yandex.ru

Чекмарева Ирина Александровна, д-р биол. наук;
ORCID: 0000-0003-0126-4473;
eLibrary SPIN: 5994-7650;
e-mail: chia236@mail.ru

Козлова Мария Александровна, канд. биол. наук;
ORCID: 0000-0001-6251-2560;
eLibrary SPIN: 5647-1372;
e-mail: ma.kozlova2021@outlook.com

Арешидзе Давид Александрович, канд. биол. наук;
ORCID: 0000-0003-3006-6281;
eLibrary SPIN: 4348-6781;
e-mail: labcelpat@mail.ru

Щедрина Марина Анатольевна, канд. мед. наук;
ORCID: 0000-0002-4265-012X;
eLibrary SPIN: 1441-7163;
e-mail: Schcedrina-m@mail.ru

Онницев Игорь Евгеньевич, д-р мед. наук;
ORCID: 0000-0002-3858-2371;
eLibrary SPIN: 9659-4740;
e-mail: ionnicev@mail.ru